Bioinorganic Chemistry

DOI: 10.1002/ange.200500338

The Hierarchical Architecture of Nacre and Its Mimetic Material**

*Yuya Oaki and Hiroaki Imai**

Biominerals fascinate many researchers because of their seemingly well-designed morphologies and hierarchical structures, which provide versatile properties.[1–4] The architecture emerging from self-organization under ambient conditions provides a sophisticated model for materials science. The design of nanostructured materials with tailored morphologies, such as particles, rods, wires, tubes, and sheets, has attracted much interest because of their potential as functional materials. Controlled assembly into a three-dimensional architecture is an important challenge in the broad application of these materials.

Living organisms make up hierarchically organized materials through self-organization from precursors in aqueous solution, and scientists have developed various biomimetic techniques to prepare and organize building blocks.[5,6] It is believed that an exquisite association of organic and inorganic compounds is required for the construction of bioinorganic superstructures; therefore, understanding the roles of macromolecules in the biomineralization process is a significant challenge in biomimetic materials chemistry. Recent findings, for example, the discovery of calcitic microlenses in brittlestars,[2] chiral morphologies with stereochemical recognition,[3] and the handedness of a snail's shell,[4] bring out hidden elaborate structures and properties of biominerals.

The nacreous layer (mother-of-pearl) has attracted the interest of researchers in a broad range of chemistry disciplines,[7–25] especially in terms of its detailed structure,[10,13,14] defects in different scales,[10] incorporated macromolecules,[15,16] mechanical strength,[17,18] formation mechanisms,[19,20] and mimetics.[21–25] The macroscopic assembly and orientation of aragonite plates, 200–600-nm thick, has been well investigated.[7–11] Although the presence of nanoscopic surface roughness and nanograins was implied in microscopic units reported previously,[13,14,18] morphology and orientation

[*] Y. Oaki, Prof. H. Imai
Department of Applied Chemistry
Faculty of Science and Technology
Keio University
3-14-1 Hiyoshi, Kohoku-ku, Yokohama, 223-8522 (Japan)
Fax: (+81) 45-566-1551
E-mail: hiroaki@applc.keio.ac.jp

[**] This work was supported by a Grant-in-Aid for Scientific Research (No. 15560587) and the 21st Century COE program "KEIO Life Conjugated Chemistry" from the Ministry of Education, Culture, Sports, Science, and Technology, Japan. We thank Mikimoto Pearl Museum for kindly providing nacre samples. Y. O. is grateful for a JSPS research fellowship for young scientists.

Supporting information for this article is available on the WWW under http://www.angewandte.org or from the author.

of the subunits were not clearly demonstrated. The emergent function resulting from an aragonite–biopolymer nanohybrid has never been investigated. An understanding of the real hierarchically organized structure in biominerals is required to advance to the next stage of chemistry, biology, and materials science.

In this study, we show that the nacreous layer is a three-level hierarchical architecture associated with two forms of oriented assembly (Figure 1). Electron microscope analysis determined the morphology of the nanobuilding blocks and their oriented assembly into platy units. Storage, an additional nanoscopic function leading to the incorporation of versatile organic dye molecules, is attributed to the aragonite–biopolymer nanohybrid. Our results are beneficial to the understanding of the overall architecture in the nacreous layer from the nanoscopic to the macroscopic scale. In addition, we demonstrate herein that an organized architecture similar to a real nacreous layer emerged from potassium sulfate (K_2SO_4) in the presence of poly(acrylic acid) (PAA; Figure 2).

Although the formation of mother-of-pearl requires several macromolecules, the two roles of PAA make up the mimetic architecture through oriented assembly. The K_2SO_4–PAA composite also generates nanostorage for the inclusion of organic dye molecules, as is the case with the nacreous layer. To gain a more comprehensive understanding of the superstructures, we show the detailed structures of two hierarchical architectures that have "nanostorage" properties and discuss the mutual growth process associated with the two respective roles of each polymer. The results imply that the manipulation of crystals and polymers could lead to a novel type of excellent inorganic–organic hybrid composites under ambient conditions.

We investigated the nacreous layer (Japanese pearl oyster: *Pinctada fucata* and its artificially induced pearl) by using field-emission scanning electron microscopy (FESEM), field-emission transmission electron microscopy (FETEM) with selected-area electron diffraction (SAED), and powder X-ray diffraction (XRD). In previous studies,[13,14] special techniques were used for FESEM and FETEM. In this study, fractured samples were used for the investigation of the actual nanoscopic structures and morphologies.[26]

As shown in Figure 1 a–h, mother-of-pearl has a hierarchical structure, with tiers 1–3 mediating the oriented assembly in two ways. As previously reported,[7–12] the layered structure (tier 1, Figure 1 a,d) consists of aragonite plates (tier 2, Figure 1 b,e) that are about 1–5-μm wide and 200–700-nm thick. The magnified FESEM image (Figure 1 b) clearly indicates the presence of smaller components in each aragonite plate. We took an FETEM image of such a nanobuilding block, which had the pseudohexagonal habit of aragonite (tier 3, Figure 1 c,f). The appearance of the nanobuilding blocks was neither attributable to the sample preparation process nor to radiation damage arising from FETEM as preceding FESEM clearly showed the presence of nanobuilding blocks in a plate (see Supporting Information). The high-resolution image on the fringe of the nanobuilding block shows a lattice spacing of 0.423 nm, which corresponds to the (110) plane of aragonite (see Supporting Information). The lengths of the nanobuilding blocks were in the range of

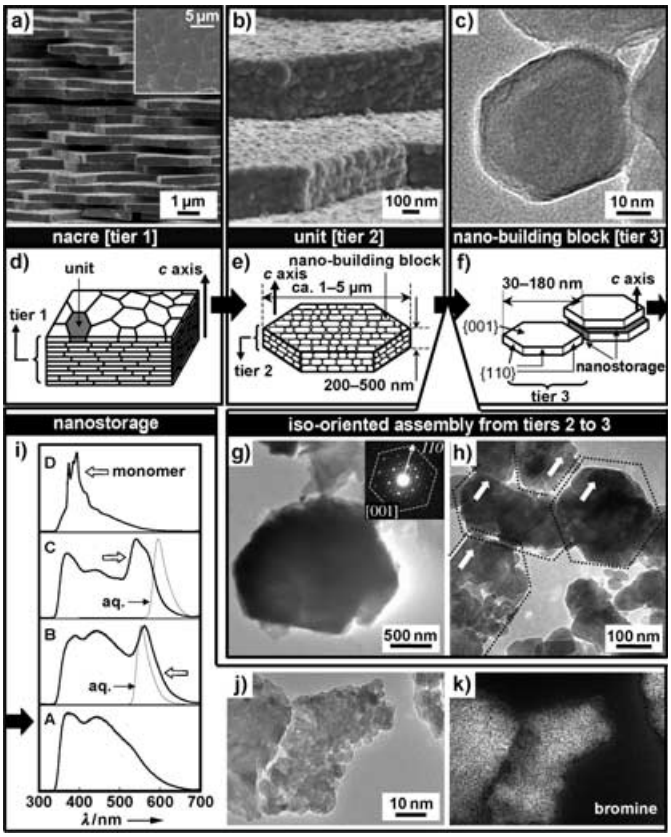

Figure 1. Hierarchically organized structure of the nacreous layer. a,b) FESEM and c) FETEM images of tiers 1–3; d–f) schematic representations of tiers 1–3; g, h) FETEM images with an SAED pattern indicating that the oriented assembly of the nanobuilding blocks make up a unit; i) photoluminescence spectra of comminuted powder of the nacreous layer (A) and with incorporation of EY (B), RB (C), and PY (D) with excitation at 290 nm; j,k) FETEM and corresponding EFTEM mapping image of the aragonite–biopolymer composite with the incorporation of EY. The bromine substituent in the EY molecule was mapped by using an energy-filtering technique.

20–180 nm, whereas the nanobuilding blocks in the mother-of-pearl shell of the oyster were smaller (see Supporting Information).

Oriented assembly mediated the formation of the hierarchical architecture. We consider the layered structure of mother-of-pearl (tier 1) to be an oriented assembly of the aragonite units (tier 2) along the *c* axis (Figure 1 d), although the orientation of the *a* and *b* axes in a layer remains unclear. The mineral-bridges model of Schäffer et al. implies that the *a* and *b* axes should be perfectly oriented in all the layers in tier 1.[19,20] However, DaiMasi and Sarikaya recently reported dark-field TEM images showing that the *a* and *b* axes were not perfectly aligned in all the layers.[11] Our XRD analysis indicates that the layers are perpendicular to the *c* axis (Supporting Information). Consequently, the oriented assembly of the plates (tier 2) in the *c* axis make up the layered structure (tier 1). A single unit (tier 2) is also an oriented assembly of nanobuilding blocks (tier 3). The SAED pattern of the fragment of a unit is spotted, which indicates that the inside of a unit is a highly aligned assembly of nanobuilding blocks (Figure 1 g). Aggregations of the nanobuilding blocks

that exhibit a hexagonal habit are commonly observed and are roughly arranged in the same direction (Figure 1 h). The peak broadening due to the crystallite-size effect is not recognizable in the XRD profiles of the powdered sample (Supporting Information). These results support the idea that the nanobuilding blocks (tier 3) generate a unit (tier 2) with oriented assembly. This concept has been implied in previous reports,[13,14] but the presence of nanobuilding blocks and their assembly were unclear.

Powdered samples of the nacreous layer were immersed in ethanol solutions of organic dyes for one day. Anionic dyes, eosin Y (EY) and rhodamine B (RB), and a hydrophobic dye, pyrene (PY), were introduced into samples of the aragonite–biopolymer composite (see Supporting Information). The resulting powders were washed with acetone and dried at room temperature. Photoluminescence spectroscopy revealed an emission from each of the included dye molecules upon excitation with UV light (Figure 1 i, white arrows); these spectra show that the aragonite–biopolymer composite incorporated not only hydrophilic but also hydrophobic dyes, such as PY. The luminescence of the aragonite–biopolymer composite was blue, as previously reported (spectrum A, Figure 1 i).[25] The aragonite–biopolymers with EY, RB, and PY incorporated gave strong orange, yellow, and blue luminescence, respectively (spectra B–D, Figure 1 i), which suggests that the EY molecules formed a J aggregate[27] and the PY molecules were included as a monomer,[28] whereas the inclusion of the RB molecules is unclear.

The incorporation of dye molecules suggests that an additional nanoscopic function resides in the aragonite–biopolymer composite. To investigate the dispersion and inclusion behavior of the EY molecules, we next performed FETEM with energy-filtered mapping (EFTEM) and electron energy-loss spectroscopy (EELS). The bromine substituents in the EY molecules were apparent in the EELS spectra (see Supporting Information) and EFTEM images (Figure 1 j,k). The images suggest that the EY molecules were homogeneously dispersed and incorporated into the aragonite–biopolymer composite on a nanoscopic scale. In the case of RB and PY, similar homogeneous incorporation leads to a strong emission. These results indicate that the aragonite–biopolymer composite behaves as a host for organic molecules. We have called this property "nanostorage".

We found that a nacre-mimetic architecture with hierarchy and nanostorage was formed spontaneously from a precursor solution containing K_2SO_4 and PAA under ambient conditions (Figure 2). Herein, we clarify the structural analogy between the K_2SO_4–PAA composite and natural mother-of-pearl. The layered morphology of the prepared material is composed of platy units (tier 1, Figure 2 a,d) that are about 0.5–1.0-μm thick (tier 2, Figure 2 b,e). The layered architecture (tier 1) is an oriented assembly of smaller units (tier 2) along the *b* axis (Figure 2 d,e); the top face of the layered structure and the unit were inferred to be the (010) face through XRD and SAED analyses. The *a* and *c* axes also align in the layered structure in tier 1, as was the case in our previous study.[29] Further FETEM observation shows that nanobuilding blocks 20 nm in diameter (tier 3, Figure 2 c,f) made up a unit (tier 2, Figure 2 b,e). FESEM and FETEM

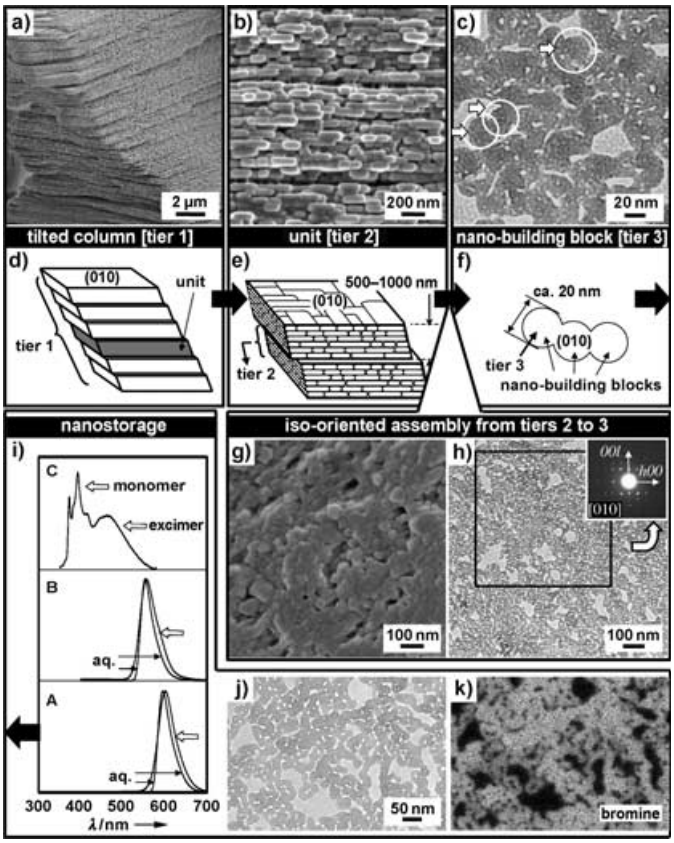

Figure 2. Hierarchically organized structure on a K_2SO_4–PAA composite. a,b) FESEM and c) FETEM images of tiers 1–3; d–f) schematic representations of tiers 1–3; g, h) FESEM and EFTEM images with an SAED pattern indicating that the oriented assembly of the nanobuilding blocks make up a unit; i) photoluminescence spectra of the nacreous layer with the inclusion of RB (A), EY (B), and PY (C) with excitation at 290 nm; j, k) FETEM and corresponding EFTEM mapping image of the K_2SO_4–PAA composite with the incorporation of EY, similar to those of the nacreous layer shown in Figure 1.

images show that the inside of a unit is an aggregate of nanobuilding blocks (Figure 2 g,h). The corresponding SAED pattern is spotted, which results from the oriented assembly of nanobuilding blocks (inset of Figure 2 h). Because peak broadening was not recognizable in the XRD profile of the powdered sample (Supporting Information), we concluded that the unit, like the nacreous layer, is an oriented assembly of nanobuilding blocks.

Dye molecules were homogeneously introduced by two methods. In the first method, EY and RB molecules were dissolved in the precursor solution and incorporated into a sample of the K_2SO_4–PAA composite as the crystals grew. In the second method, the resultant K_2SO_4–PAA composite was immersed in an ethanol solution of EY, RB, or PY. Photoluminescence spectra of samples with PY incorporated by the second method, EY incorporated by the first method, and RB also incorporated by the first method are given in Figure 2 i. On the basis of a comparison of these spectra with previously reported ones,[27,30] we surmise that EY and RB molecules organize into a J aggregate within the K_2SO_4–PAA compo-

sites (spectra A and B, Figure 2i). The incorporated PY molecules exhibit monomer and excimer emissions around 392 and 466 nm, respectively (spectrum C, Figure 2i).[28] Results obtained by FETEM, EFTEM, and EELS also suggest the homogeneous incorporation of EY molecules on a nanoscopic scale (Figure 2j,k and Supporting Information). Therefore, we concluded that, as in the case of the nacreous layer, the K_2SO_4–PAA composite has nanostorage properties.

The mutual growth process associated with the organic polymers lies in the hierarchical structures. Two types of polymers (types I and II) are required for the construction of these architectures (Figure 3a). Soluble and insoluble organic

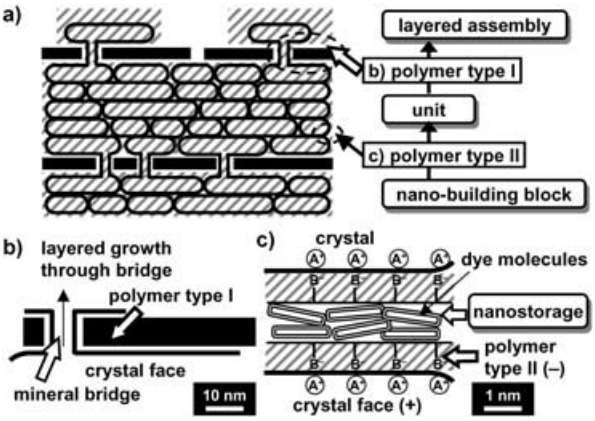

Figure 3. Schematic illustration of the mutual formation process for both the nacreous layer and the K_2SO_4–PAA composite. a) Overview of the architectures associated with polymers I and II; b) the role of polymer I: growth inhibition and subsequent promotion through the formation of a mineral bridge by polymer II; c) the role of polymer II: the control of polymorphism, crystal size, and incorporation of organic molecules (nanostorage).

molecules that are incorporated into the nacreous layer play the two respective roles in the mineralization process.[8–12,15,16] Since chitin and hydrophobic proteins (type I) form the layered sheets,[19,20] a unit eventually forms that inhibits further growth. The next layer is induced by the formation of a mineral bridge through a small pore in the sheets (Figure 3b).[19,20] The soluble acid proteins (type II) that consist of amino acids with carboxy and hydroxy groups strongly interact with carbonate crystals and produce miniaturized nanobuilding blocks, which have controlled polymorphism and orientation (Figure 3a,c). The nacre-mimetic K_2SO_4–PAA architecture is similarily caused by the two respective roles of the PAA molecules.[29] The strongly interacting PAA molecules (type II) form the nanobuilding blocks and direct the oriented assembly in tiers 2 and 3. The excess PAA molecules (type I) concurrently limit the diffusion of K^+ and SO_4^{2-} ions and inhibit further growth, so a platy unit is eventually formed (Figure 3b). However, growth is not perfectly inhibited by the PAA molecules. After the concentrations of K^+ and SO_4^{2-} ions recover around the surface of a platy unit, the next layer is mediated through the formation of a mineral bridge. The mineral bridge can be seen in the magnified FESEM image.[31]

In this way, the macroscopic periodic architecture is ascribed to the repetition of growth inhibition and subsequent restarting of the growth process. Switching between the two growth modes results in the generation of platy units and their layered assembly in tiers 1 and 2. An increase in the initial PAA concentration strongly affects the assembly of the units (tier 1),[29] whereas the morphologies in the nanoscopic architectures in tiers 2 and 3 are not much influenced. These results support the two roles played by the PAA molecules in the mineralization process. Nanostorage for organic molecules is generated by electrostatic interactions between the crystals and type II polymer because the carbon main chains not related to any interaction with crystals provide an appropriate nanoscopic environment (Figure 3c). The emergence of a hierarchical architecture associated with the respective roles of polymers can be summarized as follows: type I polymer generates the miniaturized nanobuilding blocks, which strongly interact with the crystals, and subsequently mediates the oriented assembly in a platy unit. Since the consecutive growth is inhibited by type II polymer, a layered assembly is eventually produced through the formation of a mineral bridge. These two types of polymers are combined in the crystal-growth process of real mother-of-pearl and its mimetic material. Moreover, the hierarchy in a bioinorganic superstructure emerges from the two types of polymers that fulfill the respective roles in the mineralization process.

In summary, we have elucidated the hierarchical architecture in nacre and identified its ability to host organic molecules, which we have termed "nanostorage". A nacre-mimetic architecture in terms of hierarchy, oriented assembly, and nanostorage has been generated through biomimetic crystallization of K_2SO_4 and PAA. This model case suggests that a hierarchy similar to that of nacre can be induced through an appropriate combination of inorganic crystals and organic polymers. The specific interaction of the two components generates the nanoscopic architecture, and the switching between the modes of growth leads to the formation of macroscopic structure. Furthermore, an improved understanding of real and mimetic biominerals holds promise for the further development of chemical, biological, and materials sciences.

Experimental Section

Nacreous layer: Samples of nacre comminuted by mortar were used without further washing. For the incorporation of organic dyes, nacreous powder (0.03 g) was immersed in an ethanolic solution of RB (0.2 mM), EY (0.2 mM), or PY (10 mM). The reaction mixture was subjected to ultrasound for 30 min, then left at 25 °C for 24 h. The resulting powder was isolated by centrifugation and washed with acetone.

K_2SO_4–PAA composite: A stock solution (100 g dm^{-3}) of K_2SO_4 (Kanto Chemical, 99.0%) was prepared with purified water (0.01 dm^3) at room temperature. An aqueous solution of PAA (Aldrich Chemicals, 35 wt% aqueous solution, $\bar{M}_w = 25000$) was added to the stock solution and the PAA concentration was adjusted to 10 g dm^{-3}.[29] After these materials had completely dissolved, the

sample bottle of the precursor solution was maintained at 25 °C for several days without sealing. Crystal growth proceeded as water evaporated from the solution. The soluble dye molecules EY and RB were preliminarily dissolved in the stock solution and the concentration was adjusted to 0.2 mM. Introduction of PY was carried out by the same method as that described for the nacreous layer.

Characterization: The morphologies were observed by FESEM (FEI Sirion, operating at 2.0 kV) and FETEM (FEI Tecnai F20, equipped with an energy filter (Gatan Imaging Filter), operating at 200 kV). The samples for FESEM were coated by ultrathin osmium films (plasma osmium coater, HPC-1S, Vacuum Device). For FETEM, the powder samples were added in dehydrated ethanol or purified water and subjected to ultrasound for 30 min to ensure a good dispersion. The dispersion liquid was dropped on a cupper grid. XRD was performed by using an X-ray powder diffractometer with $Cu_{K\alpha}$ radiation (XRD, Rigaku RAD-C, $2\theta/\theta$ scanning). The photoluminescence spectra were measured at room temperature by using a Shimadzu RF-5300PC spectrofluorophotometer with a xenon lamp (150 W) as the light source.

Received: January 28, 2005
Revised: June 26, 2005
Published online: September 15, 2005

Keywords: bioinorganic chemistry · biomimetic synthesis · crystal growth · organic–inorganic hybrid composites · self-assembly

[1] a) S. Mann, *Biomineralization*, Oxford University Press, Oxford, **2001**; b) S. Mann, *Angew. Chem.* **2000**, *112*, 3532–3548; *Angew. Chem. Int. Ed.* **2000**, *39*, 3392–3406; c) S. Weiner, L. Addadi, *J. Mater. Chem.* **1997**, *7*, 689–702; d) L. Addadi, S. Weiner, *Angew. Chem.* **1992**, *104*, 159–176; *Angew. Chem. Int. Ed. Engl.* **1992**, *31*, 153–169.

[2] J. Aizenberg, A. Tkachenko, S. Weiner, L. Addadi, G. Hendler, *Nature* **2001**, *412*, 819–822.

[3] a) R. M. Hazen, D. S. Sholl, *Nat. Mater.* **2003**, *2*, 367–374; b) L. Addadi, S. Weiner, *Nature* **2001**, *411*, 753–755, and references therein.

[4] a) R. Ueshima, T. Asami, *Nature* **2003**, *425*, 679; b) Y. Shibazaki, M. Shimizu, R. Kuroda, *Curr. Biol.* **2004**, *14*, 1462–1467.

[5] a) S. H. Yu, H. Cölfen, *J. Mater. Chem.* **2004**, *14*, 2124–2147; b) E. Dujardin, S. Mann, *Adv. Mater.* **2002**, *14*, 775–788; c) M. Antonietti, G. A. Ozin, *Chem. Eur. J.* **2004**, *10*, 28–41; d) H. Cölfen, S. Mann, *Angew. Chem.* **2003**, *115*, 2452–2468; *Angew. Chem. Int. Ed.* **2003**, *42*, 2350–2365, and references therein.

[6] a) Y. Oaki, H. Imai, *J. Am. Chem. Soc.* **2004**, *126*, 9271–9275; b) H. Imai, Y. Oaki, *Angew. Chem.* **2004**, *116*, 1387–1392; *Angew. Chem. Int. Ed.* **2004**, *43*, 1363–1368; c) Y. Oaki, H. Imai, *Cryst. Growth Des.* **2003**, *3*, 711–716.

[7] N. Watabe, *J. Ultrastruct. Res.* **1965**, *12*, 351.

[8] T. Kato, A. Sugawara, N. Hosoda, *Adv. Mater.* **2002**, *14*, 869–877.

[9] T. Kato, *Adv. Mater.* **2000**, *12*, 1543–1546.

[10] M. Sarikaya, *Microsc. Res. Tech.* **1994**, *27*, 360–375.

[11] E. DaiMasi, M. Sarikaya, *J. Mater. Res.* **2004**, *19*, 1471–1476.

[12] P. Calvert, S. Mann, *J. Mater. Res.* **1988**, *3*, 3801–3815.

[13] X. Li, W. C. Chang, Y. J. Chao, R. Wang, M. Chang, *Nano Lett.* **2004**, *4*, 613–617.

[14] K. Takahashi, H. Yamamoto, A. Onoda, M. Doi, T. Inaba, M. Chiba, A. Kobayashi, T. Taguchi, T. Okamura, N. Ueyama, *Chem. Commun.* **2004**, 996–997.

[15] B. A. Gotliv, L. Addadi, S. Weiner, *ChemBioChem* **2003**, *4*, 522–529.

[16] Y. L. Kalisman, G. Falini, L. Addadi, S. Weiner, *J. Struct. Biol.* **2001**, *135*, 8–17.

[17] A. P. Jackson, J. F. V. Vincent, R. M. Turner, *Proc. R. Soc. London Ser. B* **1988**, *234*, 415–440.

[18] R. Z. Wang, Z. Suo, A. G. Evans, N. Yao, I. A. Aksay, *J. Mater. Res.* **2001**, *16*, 2485–2493.

[19] L. Addadi, S. Weiner, *Nature* **1997**, *389*, 912–913.

[20] T. E. Schäffer, C. Ionescu-Zanetti, R. Proksch, M. Fritz, D. A. Walters, N. Almqvist, C. M. Zaremba, A. M. Belcher, B. L. Smith, G. D. Stucky, D. E. Morse, P. K. Hansma, *Chem. Mater.* **1997**, *9*, 1731–1740.

[21] N. Hosoda, A. Sugawara, T. Kato, *Macromolecules* **2003**, *36*, 6449–6452.

[22] N. Hosoda, T. Kato, *Chem. Mater.* **2001**, *13*, 688–693.

[23] A. Sugawara, T. Ishii, T. Kato, *Angew. Chem.* **2003**, *115*, 5457–5461; *Angew. Chem. Int. Ed.* **2003**, *42*, 5299–5303.

[24] D. Volkmer, M. Harms, L. Gower, A. Ziegler, *Angew. Chem.* **2005**, *117*, 645–650; *Angew. Chem. Int. Ed.* **2005**, *44*, 639–644.

[25] a) T. Miyoshi, Y. Matsuda, S. Akamatsu, *Jpn. J. Appl. Phys.* **1988**, *27*, 151–152; b) T. Miyoshi, Y. Matsuda, H. Komatsu, *Jpn. J. Appl. Phys.* **1987**, *26*, 578–581; c) T. Miyoshi, Y. Matsuda, H. Komatsu, *Jpn. J. Appl. Phys.* **1986**, *25*, 1606–1607.

[26] We used the fractured and the powdered samples to avoid damaging and contaminating the sample during preparation for electron microscopy analysis; the special techniques, such as focused-ion-beam, ion-milling, and microtome were not used to avoid the artifacts.

[27] a) E. Nicol, A. Moussa, J. L. Habib-Jiwan, A. M. Jonas, *J. Photochem. Photobiol. A* **2004**, *167*, 31–35; b) A. K. Dutta, C. Salesse, *Langmuir* **1997**, *13*, 5401–5408.

[28] a) A. Thomas, S. Polarz, M. Antonietti, *J. Phys. Chem. B* **2003**, *107*, 5081–5087; b) T. Förster, *Angew. Chem.* **1969**, *81*, 364–374; *Angew. Chem. Int. Ed. Engl.* **1969**, *8*, 333–343.

[29] Y. Oaki, H. Imai, *Langmuir* **2005**, *21*, 863–869.

[30] F. del Monte, D. Levy, *J. Phys. Chem. B* **1998**, *102*, 8036–8041, and references therein.

[31] The magnified FESEM images of the mineral bridge in K_2SO_4–PAA are given in the Supporting Information.

